Electronic Supplementary Information

Enhancing Performance of Organic Photovoltaic and Photodetector Devices Using Non-Atomically Doped ZnO Electrodes with Superior Optical Properties

Ziqi Su[1], Hailin Pan[1], Yi Lin[1], Zheng Li[1], Ming Wang[1,*], Zaifei Ma[1,*]

[1.] State Key Laboratory for Modification of Chemical Fibers and Polymer Materials, Center for Advanced Low-dimension Materials, College of Materials Science and Engineering, Donghua University, Shanghai 201620, China

Email: mwang@dhu.edu.cn; mazaifei@dhu.edu.cn

Keywords: *organic photovoltaics, organic photodetectors, ITO-free, non-atomically doped ZnO, optical properties*

Experimental section

Materials

Zinc acetate dihydrate ($Zn(CH_3COO)_2 \cdot 2H_2O$, 99.9%), 2-methoxyethanol ($CH_3OCH_2CH_2OH$, 99.8%), ethanolamine ($NH_2CH_2CH_2OH$, 99.5%), polyethylenimine ethoxylated (PEIE, 40 wt % in H_2O), isopropanol (IPA, 99.5%), chloroform (CF, 99.5%), chlorobenzene (CB, 99.5%), sulfuric acid (H_2SO_4) were purchased from Sigma-Aldrich. PBDB-T (poly[(2,6-(4,8-bis(5-(2-ethylhexyl)thiophen-2-yl)-benzo[1,2-b:4,5-b']dithiophene))-alt-(5,5-(1',3'-di-2thienyl-5',7'-bis (2-ethylhexyl)benzo[1',2'-c:4',5'-c']dithiophene-4,8-dione))]), PM6 (poly [(2,6-(4,8-bis (5-(2-ethylhexyl-3-fluoro) thiophene-2-yl)-benzo [1,2-b: 4,5-b'] dithiophene])-Alt-(5,5-(1' , 3'-bis-2-thiophene-5' , 7'-Bis (2-ethylhexyl) benzo [1' , 2'-C: 4' , 5'-c'] dithiophene-4,8-dione)]), PCE10 (poly [4,8-bis (5-(2-ethylhexyl) thiophenyl) benzo [1,2-b; 4,5-b'] dithiophenyl-alt-(4-(2-ethylhexyl-3-fluorothiopheno [3,4-b] thiophene -) -2-carboxylate)]), COTIC-4F (2,2'-((2Z,2'Z)-((5,5'-(4,4-bis(2-ethylhexyl)-4H-cyclopenta[1,2-b:5,4-b']dithiophene-2,6-diyl)bis(4-((2-ethylhexyl)oxy)thiophene-5,2-diyl))bis(methanylylidene))bis(5,6-difluoro-3-oxo-2,3-dihydro-1H-indene-2,1-diylidene))dimalononitrile) were procured from Solarmer Materials Inc., Beijing, ITIC (3,9-bis(2-methylene- (3-(1,1-dicyanomethylene)-indanone))-5,5,11,11-tetrakis(4-hexylphenyl)dithieno[2,3-d:2',3'-d']-s-indaceno[1,2-b:5,6-b'] dithiophene) and Y6 (2,2′-((2Z,2′Z)-((12,13-bis(2-ethylhexyl)-3,9-diundecyl-12,13-dihydro-[1,2,5]thiadiazolo[3,4-e]thieno[2,"3'':4',5']thieno[2',3':4,5]pyrrolo[3,2-g]thieno[2',3':4,5]thieno[3,2-b]indole-2,10-diyl)bis(methanylylidene))bis(5,6-difluoro-3-oxo-2,3-dihydro-1H-indene-2,1-diylidene))dimalononitrile) were purchased from Nanjing Zhiyan Technology Co. Ltd. 1,8-Diiodooctane (DIO), 1-Chloronaphthalene (CN) was acquired from Alfa Aesar. ITO glass substrates were sourced from Guangzhou Nanbo Glass Co., Ltd., while plain glass substrates were obtained from AS ONE Corp.

Fabrication of Films and Devices

The sol-gel precursor solution was prepared by mixing $Zn(CH_3COO)_2 \cdot 2H_2O$ (1.0 g), $CH_3OCH_2CH_2OH$ (10 mL) and $NH_2CH_2CH_2OH$ (277 μL). The mixture was stirred at 600 rpm for 12 hours at room temperature to ensure complete dissolution. Subsequently, the solution was filtered using a polypropylene filter with a pore size of 0.25 mm prior to utilization. Employing ambient conditions with a relative humidity ranging between 20% and 30%, a volume of 60 μL of the ZnO precursor solution was uniformly spin-coated onto a pristine glass substrate at a speed of 4000 rpm for 45 seconds. The resulting film was then subjected to annealing at 340℃ for 16 minutes. This process was iterated to deposit an additional five layers of ZnO thin films, following the same procedure. Subsequent to deposition, one half of the ZnO film underwent immersion in a dilute solution of sulfuric acid (0.1 $mol \cdot L^{-1}$) for a duration of 5 seconds, followed by thorough rinsing with ultrapure water to eliminate any residual acid from the film surface. A solution comprising 0.7 vol% of polyethyleneimine ethoxylated (PEIE) in isopropyl alcohol (IPA) was spin-coated onto the multilayered ZnO films at a speed of 5000 rpm for 60 seconds. This was succeeded by the spin-coating of the active layer atop the NAD-ZnO electrode. The active layer composed of PBDB-T:ITIC was deposited utilizing a chlorobenzene (CB) solvent, supplemented with 0.5 vol% of 1,8-diiodooctane (DIO). The solid concentration of this solution was fixed at 20 $mg \cdot mL^{-1}$, with a weight ratio of 1:1. The solution was stirring at a temperature of 70°C for 4 hours preceding its utilization. Subsequently, spin-coating was conducted at a speed of 3000 rpm for 60 seconds, followed by annealing on a hot plate at 100°C for 5 minutes. For the deposition of the active layer composed of PM6:Y6, a solution using chloroform (CF) as host solvent supplemented with a 0.5 vol% concentration of 1-Chloronaphthalene (CN) as additive. The solid concentration of this solution was adjusted to 16 $mg \cdot mL^{-1}$, with a weight ratio of 1:1.2. Similarly, for the deposition of the active layer of PCE10:COTIC-4F, the solution was prepared by stirring at 25°C for 4 hours. Spin-coating was executed at a speed of 3000 rpm for 60 seconds without subsequent annealing. The CF solution utilized for this purpose also contained a 0.5 vol% concentration of CN, with a solid concentration set to 14 $mg \cdot mL^{-1}$

and a weight ratio of 1:1.2. Following spin-coating, the film underwent annealing at 100°C for 5 minutes on a hot plate and then subjected to further processing in a vacuum evaporation chamber, maintained at a vacuum level of less than 10^{-6} mbar. In this chamber, layers of 10 nm MoO_3 layer and 100 nm Ag layer were evaporated onto the active layer film through a shadow mask.

Characterizations

The conductivity of NAD-ZnO films: Sheet resistances of the NAD-ZnO films were firstly determined using a four-point probe station, with the measured resistances recorded via a Keithley 2450 source meter and the four-point probe station used was HPS2662-type high-precision meter. Meanwhile, the thicknesses of the NAD-ZnO films were assessed by a J.A. Woollam M-2000 Spectroscopic ellipsometer. Subsequently, utilizing the conductivity calculation equation:

$$\sigma = \frac{l}{RS} = \frac{l}{Rdl} = \frac{1}{Rd}$$

the conductivity of the film was computed. Here, R is the sheet resistance, S is the cross-sectional area through which the current flows, d is the thickness of NAD-ZnO film, and l is the length of the current pathway

The absorption of the films was measured using a UV-vis spectrophotometer (Lambda 950, PerkinElmer Inc.). Subsequently, according to the equation:

$$\alpha = \frac{A}{d}$$

the absorption coefficient α was calculated. Here, d is the thickness of the films, A is the absorption.

The surface profile of the NAD-ZnO films were recorded by a step profiler (Tencor® P-7).

AFM images were recorded using an atomic force microscopy (MFP-3D-BIO™, Asylum Research).

The *J-V* curves of the OPV devices were evaluated using a standard solar

simulator (AM1.5 G, Newport Oriel VeraSol-2™ Class AAA) or a LED lamp (3000 K), while applying a bias voltage to the devices. The resulting current was measured using a Keithley 2400 source meter. Additionally, dark *J-V* curves were obtained using the same setup, but without illumination from light sources.

EQE and sEQE spectra were acquired through a home-built experimental arrangement comprising a halogen lamp (LSH-75, 250W, Newport), a monochromator (CS260-RG-3-MC-A, Newport), and an optical chopper. The organic photovoltaic device under examination was securely affixed to the apparatus stage. Illumination was provided by the halogen lamp, which emitted light directed through the monochromator, thereby generating monochromatic light with adjustable wavelength settings. This monochromatic light was then modulated into pulsed light via the optical chopper. Subsequently, the light passed through a condenser mirror and aperture, resulting in a focused and appropriately sized light spot that illuminated the device under investigation. Upon absorption of incident photons by the device, the ensuing electrical signal was captured by a front-end current amplifier (SR570, Stanford) and a lock-in amplifier (SR830, Stanford).

EQE_{EL} measurements were conducted using a custom-built setup, including a digital source meter (Keithley 2400) a silicon diode and a picoammeter (Keithley 6482). The prepared organic photovoltaic device is fixed on the device platform, and the Keithley 2400 digital source meter is used to inject current into the device. The silicon-based detector can detect the photons emitted by the device and convert them into electrical signals, which are ultimately collected by the Keithley 6842 and output as an EQE_{EL} spectrum.

EL spectra were acquired employing a comprehensive setup comprising a source meter (Keithley 2400), a fluorescence spectrometer (KYMERA-3281-B2, Andor), a silicon electron-multiplying charge-coupled device (EMCCD) camera (DU970P-BVF, Andor), and an indium gallium arsenide (InGaAs) camera (DU491A-1.7, Andor).

Current was supplied to the device via the source meter, while emitted photons weregathered utilizing optical fibers. Throughout the experimental procedure, the silicon EMCCD camera and the InGaAs camera were employed to capture photons within distinct wavelength ranges.

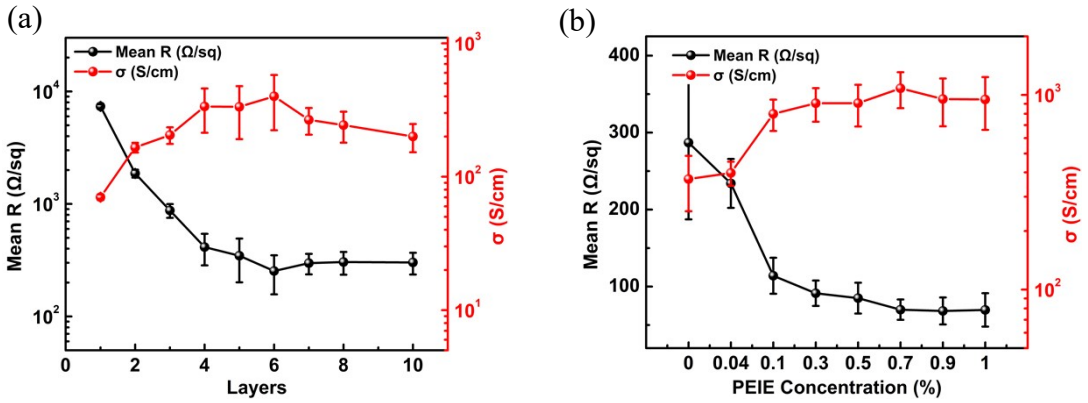

Figure S1. The resistivity and conductivity of ZnO thin films **a)** with different numbers of ZnO layers and **b)** different concentrations of polyethyleneimine ethoxylated (PEIE) treatment.

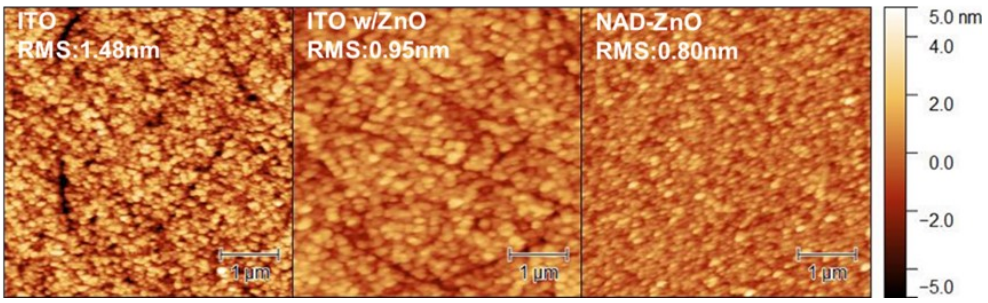

Figure S2. The AFM images for ITO, ITO/ZnO and NAD-ZnO films.

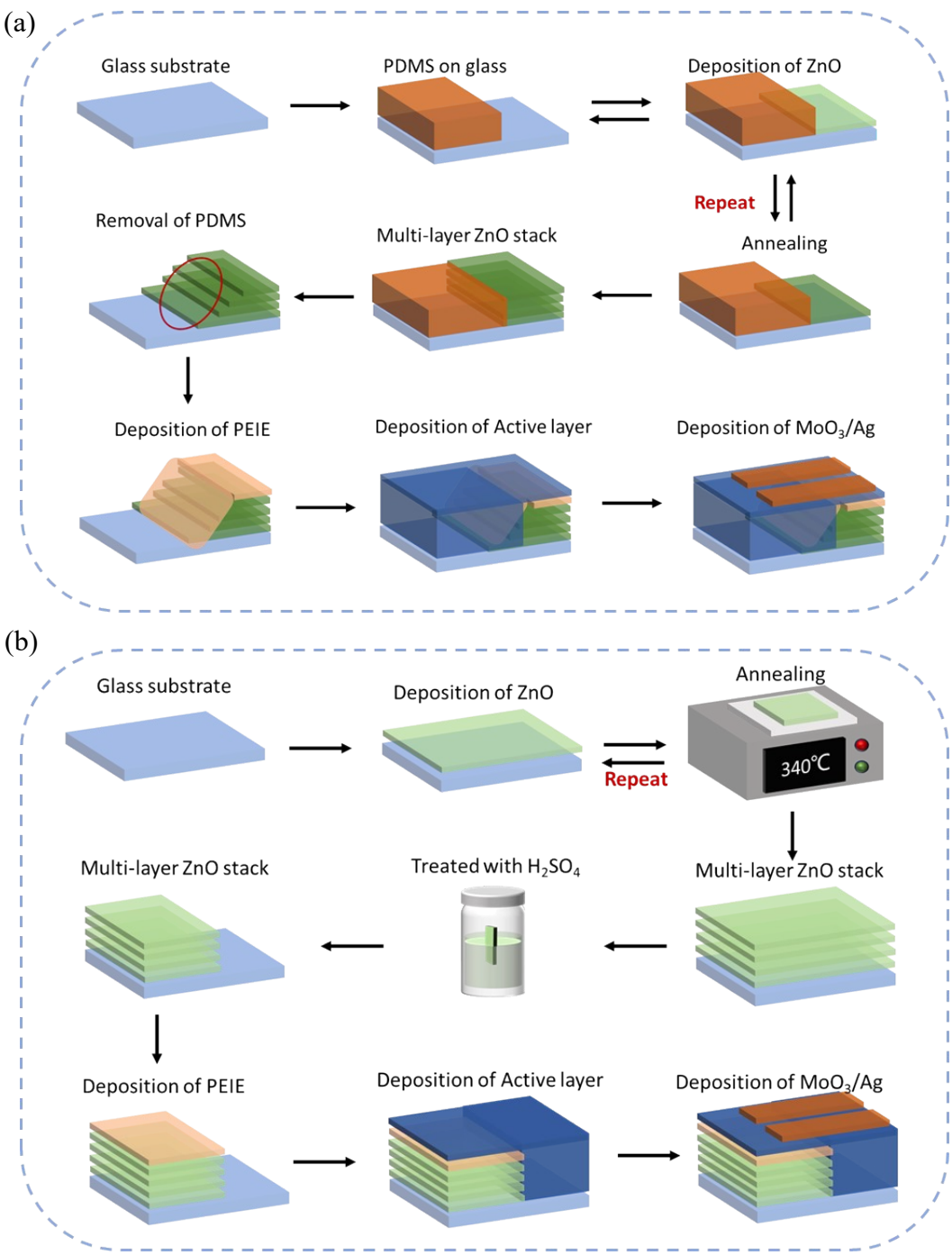

Figure S3. A schematic representation of the 6-layer NAD-ZnO electrode **a)** treated with PDMS and **b)** treated with dilute sulfur acid.

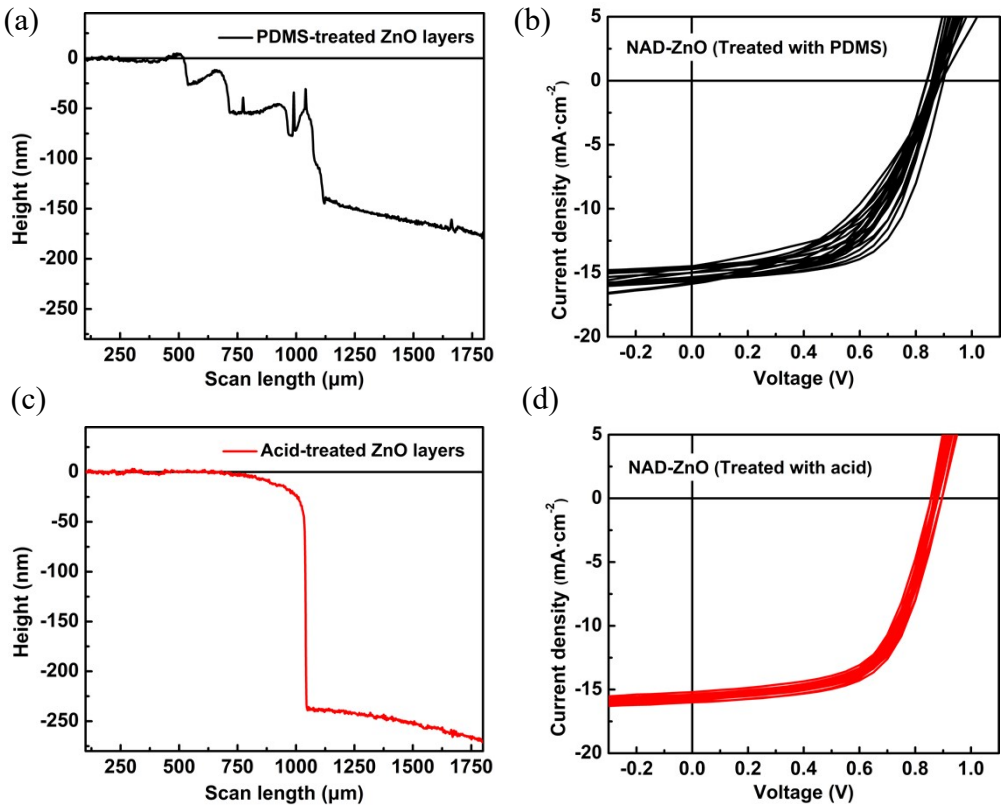

Figure S4. a) The surface profile of the NAD-ZnO electrode treated with PDMS, **b)** the *J-V* curves for the 20 NAD-ZnO-based OPV devices utilizing PDMS-treated NAD-ZnO electrodes, **c)** the surface profile of the NAD-ZnO electrode treated with acid, **d)** The *J-V* curves for the 20 NAD-ZnO-based OPV devices utilizing acid-treated NAD-ZnO electrodes.

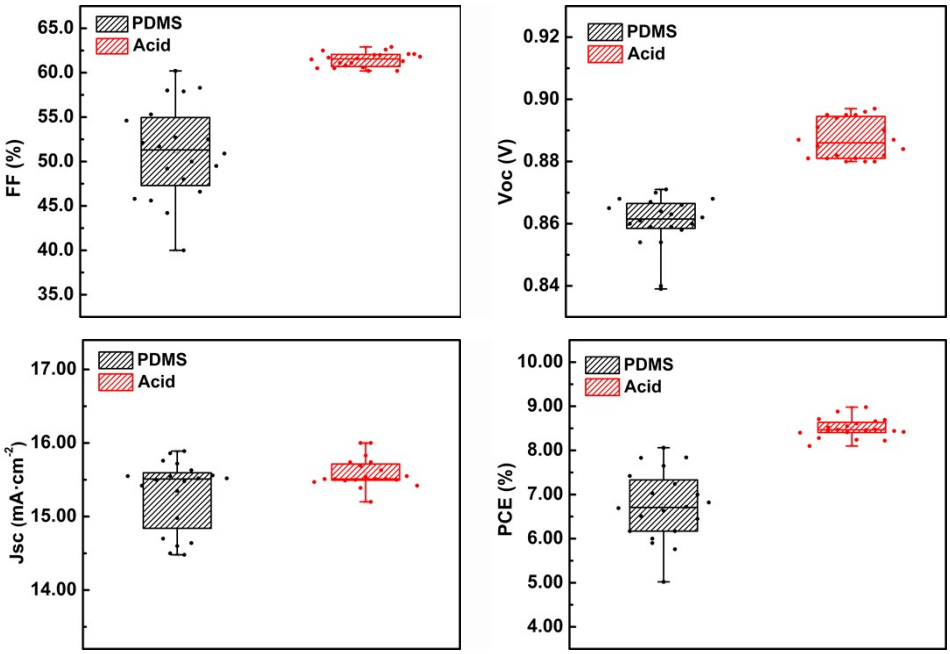

Figure S5. A statistical distribution chart illustrating the photovoltaic performance parameters in NAD-ZnO-based devices treated with PDMS and dilute sulfuric acid. The photovoltaic parameters of these devices are detailed in Table S2 and S3.

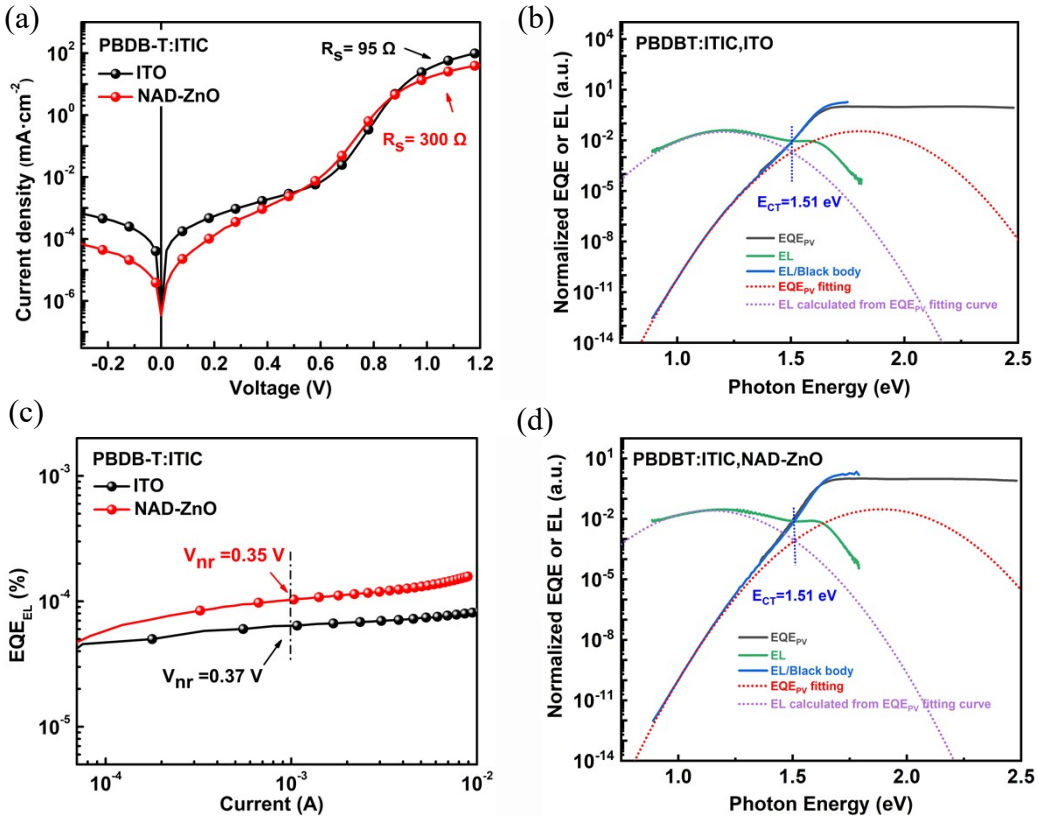

Figure S6. a) The dark *J-V* curves, **b)** sEQE and EL spectra, **c)** EQE_{EL} *versus* injected current curves and **d)** sEQE and EL spectra for the determination of E_{CT}, using the method described in the literature (*J. Mater. Chem. A*, 2021, **9**, 19770–19777), utilizing PBDB-T:ITIC as the active layer.

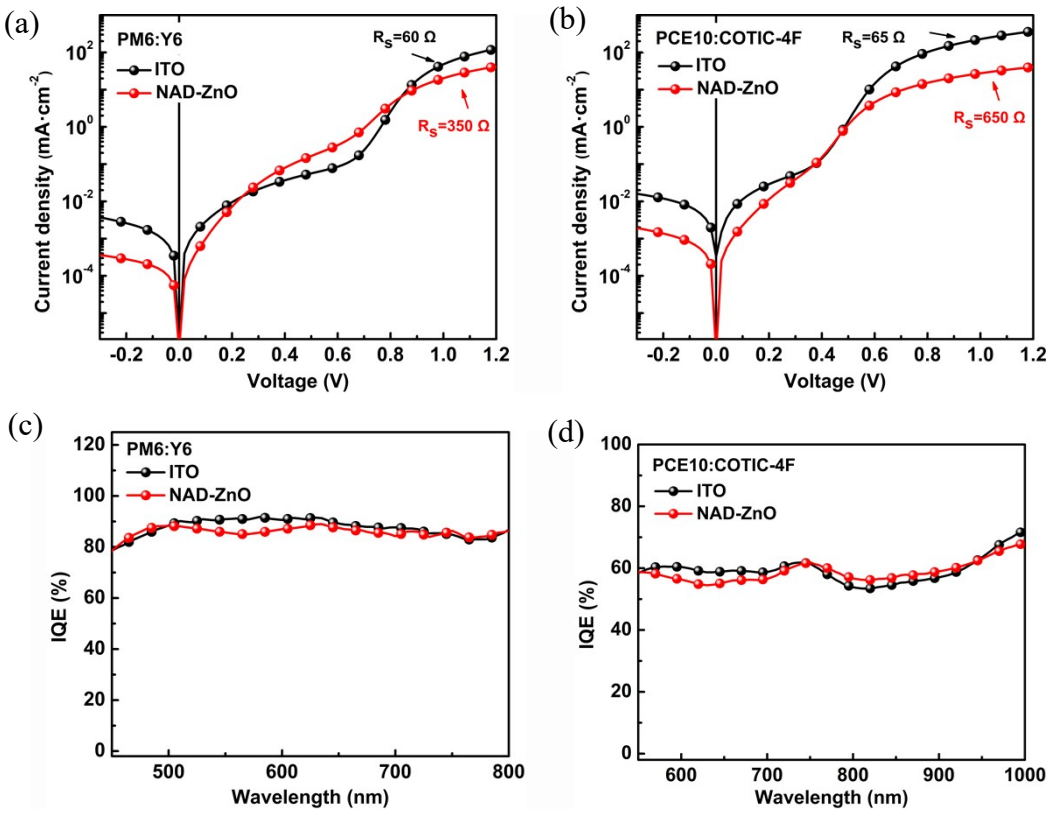

Figure S7. The dark *J-V* curves for the NAD-ZnO- and ITO-based OPV devices using **a)** PM6:Y6 and **b)** PCE10:COTIC-4F as the active layer. The IQE spectra for the NAD-ZnO- and ITO-based OPV devices using **c)** PM6:Y6 and **d)** PCE10:COTIC-4F as the active layer.

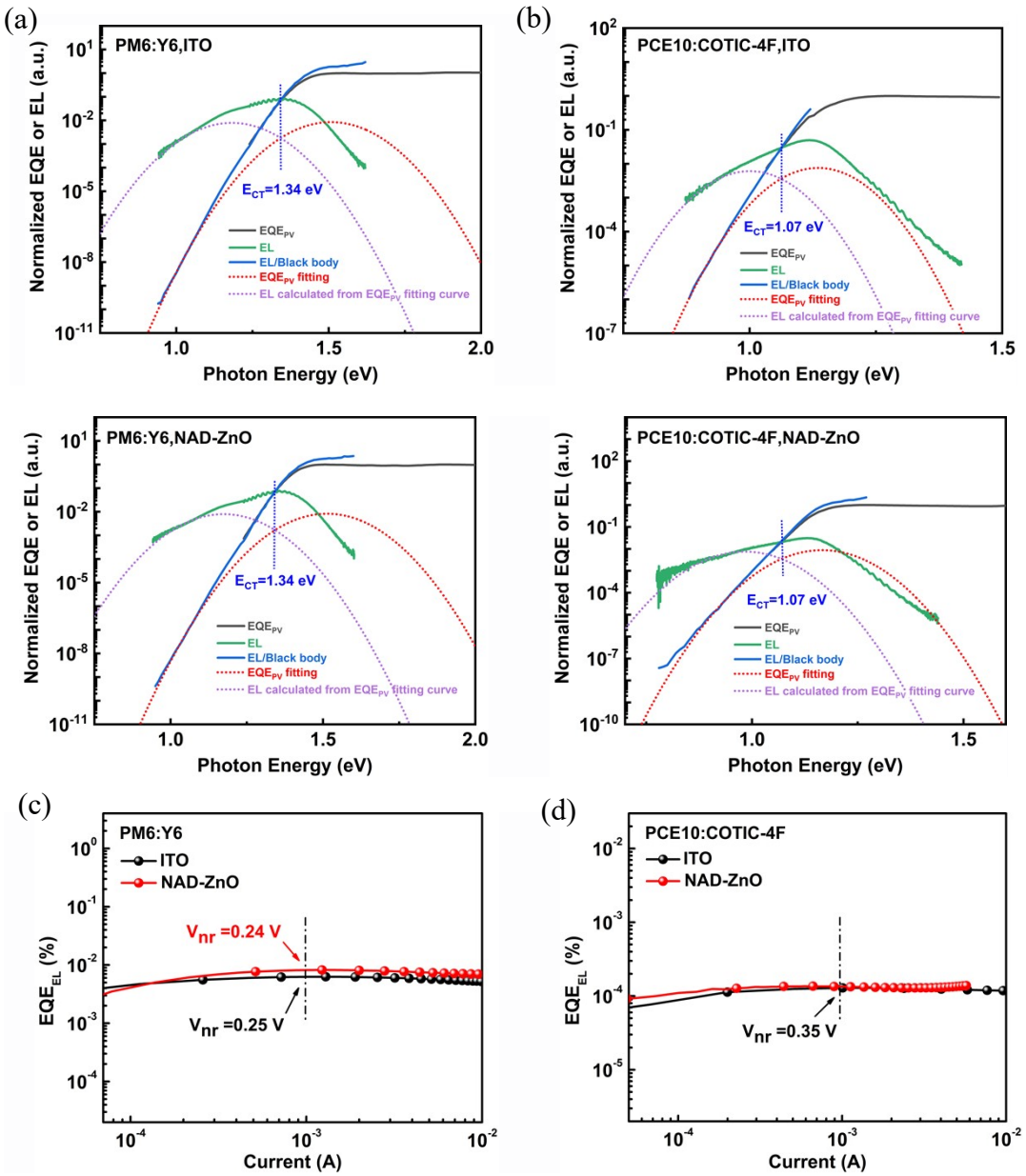

Figure S8. sEQE and EL spectra for the determination of E_{CT} for the NAD-ZnO- and ITO-based OPV devices using **a)** PM6:Y6 and **b)** PCE10:COTIC-4F as the active layer. EQE_{EL} versus injected current curves for the NAD-ZnO- and ITO-based OPV devices using **c)** PM6:Y6 and **d)** PCE10:COTIC-4F as the active layer.

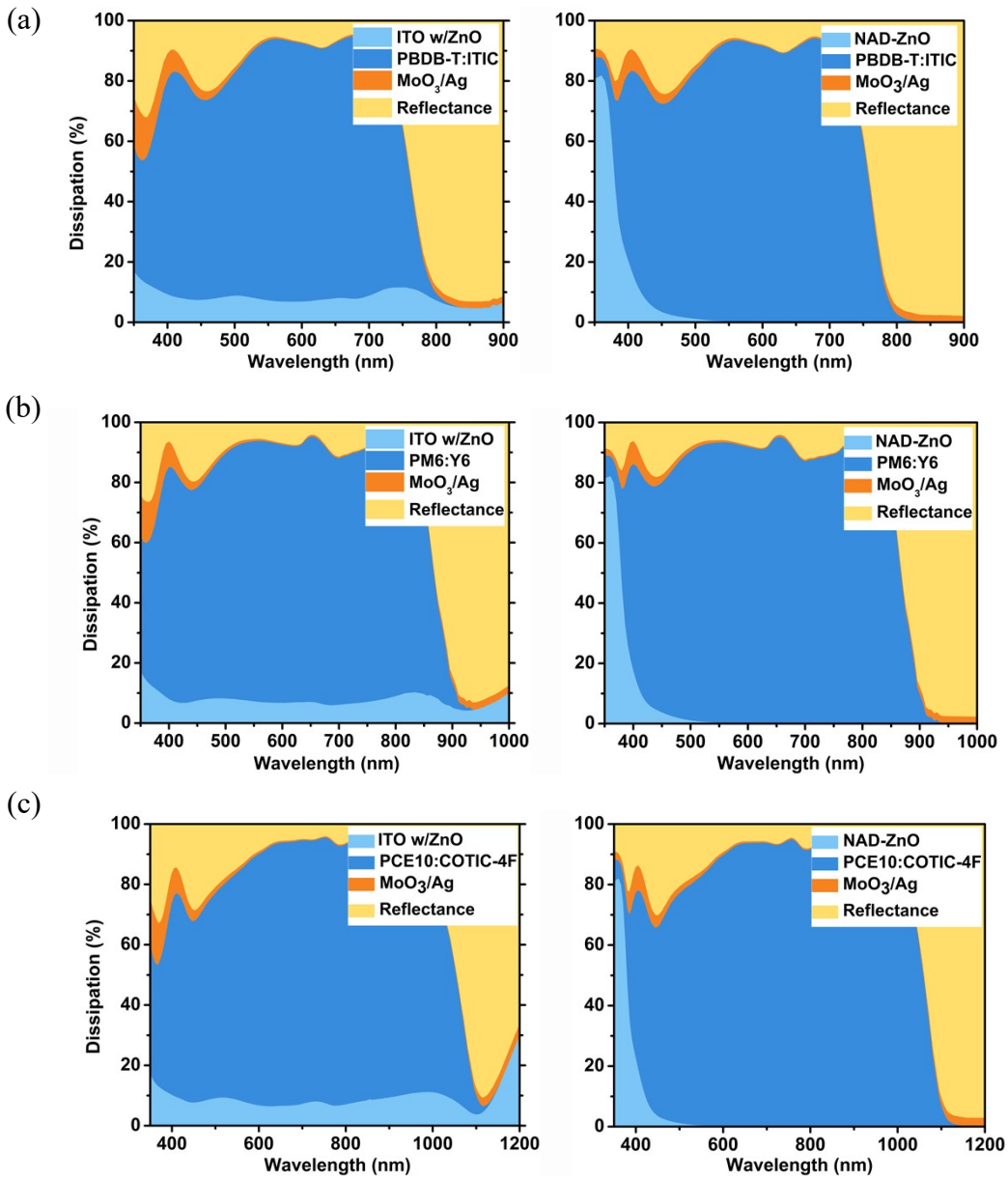

Figure S9. The TM simulated reflectance and absorptance profile for the NAD-ZnO- and ITO-based OPV devices using **a)** PBDB-T:ITIC, **b)** PM6:Y6 and **c)** PCE10:COTIC-4F as the active layer.

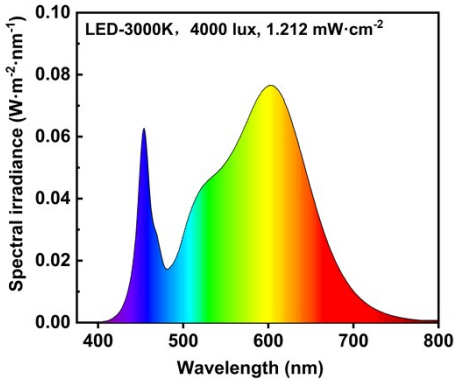

Figure S10. The emission spectrum of the LED lamp (3000 K).

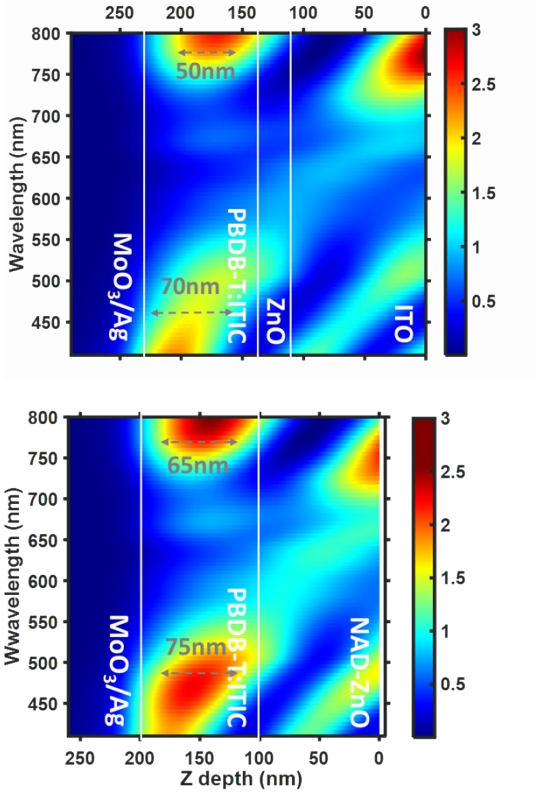

Figure S11. The optical field distribution of PBDB-T:ITIC OPV devices utilizing both NAD-ZnO and ITO electrodes, when subjected to a LED (3000 K) light source at an intensity of 4000 lux.

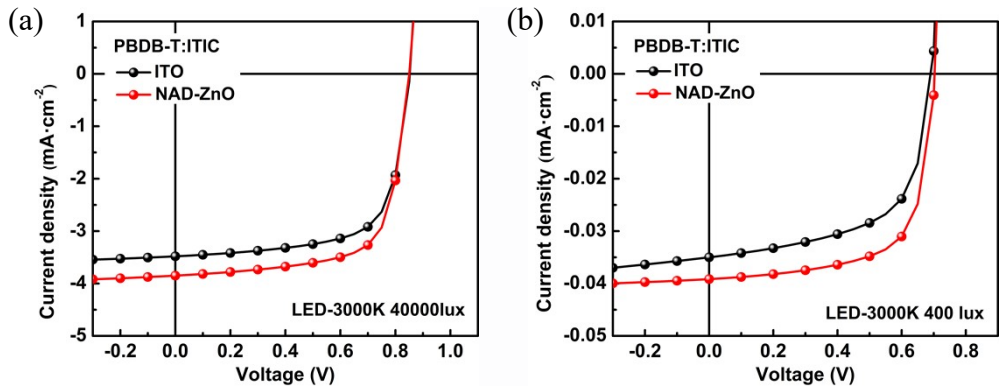

Figure S12. The *J-V* curves of PBDB-T:ITIC OPV devices, utilizing both NAD-ZnO and ITO electrodes, under a LED (3000 K) light source at an intensity of **a)** 40000 lux and **b)** 400 lux.

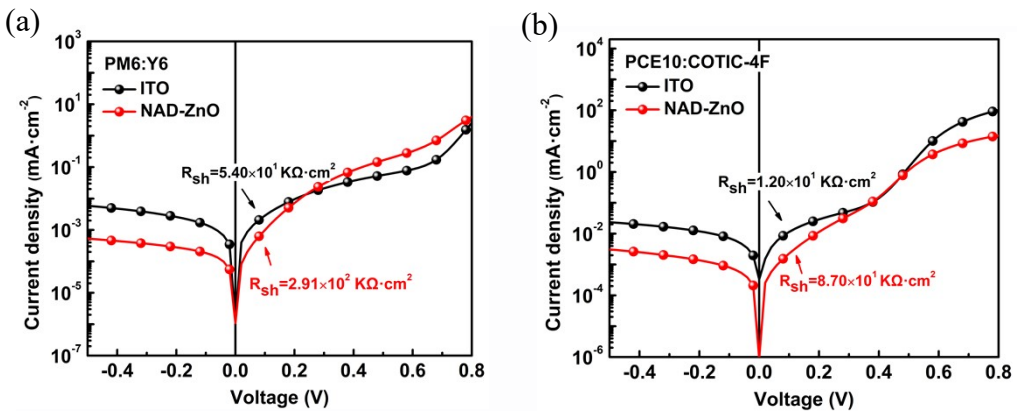

Figure S13. The dark *J-V* dark curves of **a)** PM6:Y6 and **b)** PCE10:COTIC-4F OPD devices, utilizing both NAD-ZnO and ITO electrodes.

Table S1. The representative photovoltaic performance parameters in NAD-ZnO-based devices treated with PDMS and dilute sulfuric acid.

Electrode	J_{sc} (mA·cm^{-2})	V_{oc} (V)	FF (%)	PCE (%)
PDMS-treated ZnO layers	15.31±0.47	0.86±0.01	51.2±5.3	6.7±0.8
Acid-treated ZnO layers	15.59±0.20	0.89±0.01	61.5±0.8	8.5±0.2

Table S2. The PV parameters of 20 OPV devices utilizing PDMS treated NAD-ZnO electrode.

Electrode	J_{sc} (mA·cm^{-2})	V_{oc} (V)	FF (%)	PCE (%)
PDMS-treated ZnO layers	15.89	0.86	52.7	7.2
	15.48	0.85	57.9	7.6
	15.72	0.86	58.0	7.8
	15.86	0.87	48.0	6.6
	14.48	0.87	40.0	5.0
	14.60	0.86	49.2	6.2
	15.76	0.86	51.7	7.0
	15.55	0.86	60.2	8.1
	15.35	0.84	46.6	6.0
	15.52	0.87	58.3	7.9
	15.50	0.84	50.0	6.5
	15.63	0.86	52.1	7.0
	14.98	0.85	52.5	6.7
	14.70	0.86	45.6	5.8
	15.56	0.87	49.5	6.7
	15.42	0.87	55.3	7.4
	14.50	0.86	54.6	6.8
	14.64	0.87	50.9	6.5
	15.52	0.87	45.8	6.2
	15.55	0.86	44.2	5.9

Table S3. The PV parameters of 20 OPV devices utilizing acid treated NAD-ZnO electrode.

Electrode	J_{sc} (mA·cm^{-2})	V_{oc} (V)	FF (%)	PCE (%)
Acid-treated ZnO layers	15.54	0.88	60.2	8.2
	15.50	0.90	60.6	8.5
	15.51	0.90	62.0	8.7
	15.49	0.90	61.6	8.6
	15.51	0.88	62.0	8.5
	15.51	0.89	61.1	8.4
	16.00	0.90	62.6	9.0
	15.83	0.88	60.8	8.5
	16.00	0.88	62.9	8.9
	15.74	0.88	61.1	8.5
	15.50	0.88	60.2	8.2
	15.51	0.88	60.5	8.3
	15.55	0.89	61.3	8.5
	15.69	0.90	61.7	8.7
	15.47	0.89	62.1	8.6
	15.63	0.89	62.5	8.7
	15.74	0.89	62.1	8.7
	15.20	0.88	60.5	8.1
	15.42	0.88	61.8	8.4
	15.39	0.89	61.5	8.4

Table S4. The parameters of voltage loss for ZnO- and ITO-based OPV devices, employing PBDB-T:ITIC, PM6:Y6 and PCE10:COTIC-4F as the active layer.

	Electrode	$J_{0,rad}$ [a] (mA·cm^{-2})	E_{CT} (eV)	$V_{oc,rad}$ [b] (V)	EQE_{EL} (%)	ΔV_{nr} [c] (V)	ΔV_r [d] (V)	ΔV_{loss} [e] (V)
PBDB-T:ITIC	ITO w/ZnO	1.8×10^{-20}	1.51	1.24	6.4×10^{-5}	0.37	0.35	0.72
	NAD-ZnO	1.8×10^{-20}	1.51	1.24	1.0×10^{-4}	0.35	0.35	0.70
PM6:Y6	ITO w/ZnO	2.0×10^{-17}	1.34	1.07	6.3×10^{-3}	0.25	0.26	0.51
	NAD-ZnO	2.0×10^{-17}	1.34	1.07	7.4×10^{-3}	0.24	0.26	0.50
PCE10:COTIC-4F	ITO w/ZnO	9.0×10^{-15}	1.07	0.91	1.3×10^{-4}	0.35	0.19	0.54
	NAD-ZnO	9.0×10^{-15}	1.07	0.91	1.3×10^{-4}	0.35	0.19	0.54

[a] $J_{0,rad}$ values calculated from the equation: $J_{0,rad} = q\int EQE(E)BB(E)dE$

where $BB(E)$ is the blackbody emission photon flux and E is the photon energy.

[b] $V_{oc,rad}$ values calculated from the equation: $V_{oc,rad} = \frac{kT}{q} ln(\frac{J_{sc}}{J_{0,rad}})$

where k is the Boltzmann's constant, q is the elementary charge, T is the absolute temperature and J_{sc} is the short-circuit current density.

[c] ΔV_{nr} values calculated from the equation: $\Delta V_{nr} = \frac{kT}{q} ln(\frac{1}{EQE_{EL}})$ or $\Delta V_{nr} = V_{oc,rad} - V_{oc}$

[d] ΔV_r values calculated from the equation: $\Delta V_r = \Delta V_{loss} - \Delta V_{nr}$

[e] ΔV_{loss} values calculated from the equation: $\Delta V_{loss} = \frac{E_g}{q} - V_{oc}$

Table S5. The summaries of the PV parameters of PBDB-T:ITIC OPV devices, utilizing both NAD-ZnO and ITO electrodes, under a LED (3000 K) light source with varying illumination intensities.

Electrode	P_{in}(mW·cm^{-2})	Intensity (lux)	PCE(%)	J_{sc} (mA·cm^{-2})	V_{oc} (V)	FF (%)
ITO w/ZnO	12.12	40000	16.8	3.48	0.85	68.9
	1.212	4000	14.7	0.348	0.75	68.2
	0.121	400	12.1	0.035	0.69	60.9
NAD-ZnO	12.12	40000	18.9	3.85	0.85	69.9
	1.212	4000	18.0	0.390	0.78	71.7
	0.121	400	15.3	0.039	0.70	67.6